THE JOURNAL OF BIOLOGICAL CHEMISTRY VOL. 290, NO. 25, pp. 15526–15537, June 19, 2015

Ubiquitin-specific Protease 11 (USP11) Deubiquitinates Hybrid Small Ubiquitin-like Modifier (SUMO)-Ubiquitin Chains to Counteract RING Finger Protein 4 (RNF4)*[S]

Received for publication, October 10, 2014, and in revised form, April 30, 2015 Published, JBC Papers in Press, May 12, 2015, DOI 10.1074/jbc.M114.618132

Ivo A. Hendriks[‡], Joost Schimmel[‡], Karolin Eifler[‡], Jesper V. Olsen[§], and Alfred C. O. Vertegaal[‡1]

From the [‡]Department of Molecular Cell Biology, Leiden University Medical Center, Albinusdreef 2, 2333 ZA, Leiden, The Netherlands and the [§]Novo Nordisk Foundation Center for Protein Research, Faculty of Health and Medical Sciences, University of Copenhagen, Blegdamsvej 3B, 2200, Copenhagen, Denmark

Background: RNF4 is a ubiquitin ligase targeted to SUMOylated proteins.
Results: USP11 co-purified with RNF4 and can remove ubiquitin polymers attached to SUMO chains.
Conclusion: USP11 is a ubiquitin protease with the ability to counteract RNF4 in the DNA damage response.
Significance: Identification of a ubiquitin protease to balance the activity of a SUMO-targeted ubiquitin ligase.

Ring finger protein 4 (RNF4) is a SUMO-targeted ubiquitin E3 ligase with a pivotal function in the DNA damage response (DDR). SUMO interaction motifs (SIMs) in the N-terminal part of RNF4 tightly bind to SUMO polymers, and RNF4 can ubiquitinate these polymers *in vitro*. Using a proteomic approach, we identified the deubiquitinating enzyme ubiquitin-specific protease 11 (USP11), a known DDR-component, as a functional interactor of RNF4. USP11 can deubiquitinate hybrid SUMO-ubiquitin chains to counteract RNF4. SUMO-enriched nuclear bodies are stabilized by USP11, which functions downstream of RNF4 as a counterbalancing factor. In response to DNA damage induced by methyl methanesulfonate, USP11 could counteract RNF4 to inhibit the dissolution of nuclear bodies. Thus, we provide novel insight into cross-talk between ubiquitin and SUMO and uncover USP11 and RNF4 as a balanced SUMO-targeted ubiquitin ligase/protease pair with a role in the DDR.

Small ubiquitin-like modifiers (SUMOs)[2] are predominantly located in the nucleus and play key roles in all nuclear processes including transcription, chromatin modification, and maintenance of genome stability (1). Analogous to the ubiquitin system, a set of E1, E2, and E3 enzymes mediates the conjugation of SUMO to target proteins, and a set of SUMO-specific proteases is responsible for the reversible nature of this post-translational modification (2, 3). Mouse models have shown that the SUMOylation system is essential for embryonic development. Mice deficient for the single SUMO E2 enzyme Ubc9 die at the early post-implantation stage as a result of hypocondensation and other chromosomal aberrancies (4).

Large sets of target proteins have been identified for the different SUMO family members involved in all different nuclear processes (5–7). About half of the SUMO acceptor lysines in these target proteins are located in short stretches that fit the SUMOylation consensus motif ΨK*X*E (7, 8), a motif that is directly recognized by Ubc9 (9, 10). Internal SUMOylation consensus motifs in human SUMO-2 and SUMO-3 enable SUMO polymerization (11–14). SUMO signal transduction furthermore includes proteins that bind non-covalently to SUMOylated proteins via SUMO interaction motifs (SIMs) (15), including the novel SUMO binding zinc finger identified in HERC2 (16).

Interestingly, extensive cross-talk exists between the SUMOylation system and the ubiquitination system (17, 18). This cross-talk includes competition between SUMO and ubiquitin for the same acceptor lysines (19) or sequential modification by SUMO and ubiquitin of a target protein (20). Moreover, the SUMO system is tightly connected to the ubiquitin-proteasome pathway as a significant subset of SUMO-2/3 target proteins is subsequently ubiquitinated and degraded by the proteasome (21, 22). Inhibition of the proteasome led to accumulation of SUMO-2/3 conjugates and the depletion of the pool of non-conjugated SUMO-2/3, indicating that this biochemical pathway is required for SUMO-2/3 recycling. SUMO and ubiquitin can form hybrid chains, including via lysine 32 of SUMO-2 or lysine 33 of SUMO-3 (21).

The SUMO system and the ubiquitin system are linked together via the SUMO-targeted ubiquitin ligases (STUbLs), responsible for ubiquitinating SUMOylated proteins. They were first identified in *Schizosaccharomyces pombe* as Rfp1 and Rfp2 and in *Saccharomyces cerevisiae* as the Slx5-Slx8 complex (23–25). Rfp1 and -2 each have an N-terminal SIM and a C-terminal RING finger domain to enable interaction with SUMOylated proteins. Ubiquitin E3 ligase activity of the Slx5-Slx8 complex is provided by the active RING finger protein Slx8. RNF4 is a major mammalian STUbL containing four

* This work was supported by the Netherlands Organization for Scientific Research (NWO) (to A. C. O. V.), ZonMW (to A. C. O. V.), the European Research Council (to A. C. O. V.), and the research career program FSS Sapere Aude (to J. V. O.) from the Danish Research Council. The authors declare that they have no conflicts of interest with the contents of this article.
[S] This article contains supplemental Table 1.
[1] To whom correspondence should be addressed. Tel.: 31-71-526-9621; Fax: 31-71-526-8270; E-mail: vertegaal@lumc.nl.
[2] The abbreviations used are: SUMO, small ubiquitin-like modifier; SIM, SUMO interaction motif; STUbL, SUMO-targeted ubiquitin ligase; MMS, methyl-methane sulfonate; Bis-Tris, 2-[bis(2-hydroxyethyl)amino]-2-(hydroxy methyl)propane-1,3-diol; RNF4, ring finger protein 4; IP, immunoprecipitation; USP11, ubiquitin-specific protease 11; MBP, maltose-binding protein; PML, promyelocytic leukemia protein.

N-terminal SIMs and a C-terminal RING domain that enables homodimerization (26). More recently, RNF111/Arkadia was identified as a second mammalian STUbL (27, 28).

STUbLs play key roles in the DNA damage response (29). *S. pombe* strains deficient for STUbLs display genomic instability and are hypersensitive to different DNA damaging agents including hydroxyurea, methylmethane sulfonate (MMS), camptothecin, and ultraviolet light (23, 24). RNF4 knockdown in human cells also results in increased sensitivity to DNA damaging agents (30). Moreover, RNF4 accumulates at DNA damage sites induced by laser micro-irradiation (30–32). SUMOylated target proteins for RNF4 include MDC1 and BRCA1 (32, 33) and, furthermore, HIF-2α (34). Mice deficient for RNF4 die during embryogenesis (32, 35). Mice expressing strongly reduced levels of RNF4 are born alive, albeit at a reduced Mendelian ratio, and showed an age-dependent impairment in spermatogenesis (32). MEFs derived from these mice exhibit increased sensitivity to genotoxic stress.

A key feature of ubiquitin-like modification systems is their reversible nature to carefully balance the systems (2, 36). Deubiquitinating enzymes play a pivotal role in the regulation of cellular ubiquitination levels, essentially controlling all cellular processes. Around 100 mammalian deubiquitinating enzymes exist, with different substrate specificity, subcellular localization, and protein-protein interactions (36, 37). Currently, it is not clear how the activity of the STUbLs is balanced. Here, we report the identification of a ubiquitin-specific protease with the ability to counteract RNF4.

Experimental Procedures

Plasmids—The cDNA encoding the USP11 protein was a kind gift from Dr. L. Zhang and Prof. P. ten Dijke in our institute. The cDNA encoding the RNF4 protein was obtained from the Mammalian Gene Collection (Image ID 4824114; supplied by Source Bioscience). Both cDNAs were amplified by a two-step PCR reaction using the following primers: 5′-AAAAAGCAGGCTATATGGCAGTAGCCCCGCGACTG-3′ and 5′-AGAAAGCTGGGTGTCAATTAACATCCATGAACTC-3′ (USP11), 5′-AAAAAGCAGGCTCAATGAGTACAAGAAAGC-3′ and 5′-AGAAAGCTGGGTTTCATATATAAATGGGGTG-3′ (RNF4) for the first reaction, and 5′-GGGGACAAGTTTGTACAAAAAAGCAGGCT-3′ and 5′-GGGGACCACTTTGTACAAGAAAGCTGGGT-3′ for the second reaction. RNF4 was cloned in between the SpeI and XhoI sites of the plasmid pLV-CMV-X-FLAG-IRES-GFP (a kind gift from Dr. R. C. Hoeben). Additionally, RNF4 and USP11 cDNAs were inserted into pDON207 employing standard Gateway technology (Life Technologies). The C318A mutation in USP11 was introduced by QuikChange site-directed mutagenesis (Stratagene) using oligonucleotides 5′-CAATCTGGGCAACACGGCCTTCATGAACTCGG-3′ and 5′-CCGAGTTCATGAAGGCCGTGTTGCCCAGATTG-3′. These different cDNAs were subsequently transferred to the destination vector pDEST-T7-His_6-MBP (a kind gift from Dr. L. Fradkin in our institute). RNF4 was cloned into pGEX-2T to obtain a construct encoding GST-tagged RNF4 by amplifying RNF4 cDNA using the primers 5′-ACAAACGGATCCATGAGTACAAGAAAGCGTCGTG-3′ and 5′-GCCGCGGAATTCTCATATATAAATGGGGTGGTAC-3′. Both the PCR product and the pGEX-2T vector were subsequently digested with BamHI and EcoRI, and the PCR product was ligated into the vector with T4 ligase (New England Biolabs). The His_6-ΔN11-SUMO-2-Tetramer expression vector was a kind gift of Prof. Dr. R. T. Hay (University of Dundee, UK) (26). The His_6 tag was extended to His_{10} through PCR.

Cell Culture and Cell Line Generation, Transfection, and Treatments—MCF7, U2-OS, and HeLa cells were cultured in Dulbecco's modified Eagle's medium (DMEM) supplemented with 10% FBS and 100 units/ml penicillin and streptomycin (Life Technologies). MCF7 cells stably expressing RNF4-FLAG were generated through lentiviral infection with a construct carrying RNF4-FLAG-IRES-GFP. Two weeks after infection cells were sorted for a low level of GFP by flow cytometry using a FACSAria II sorter (BD Biosciences). Cells were treated with 0.02% MMS (Sigma) for the indicated amounts of time. Transfections were performed using 2.5 μg of polyethyleneimine per 1 μg of plasmid DNA using 1 μg of DNA per 1 million cells. Transfection reagents were mixed in 150 mM of NaCl and incubated for 15 min before transfection. Cells were split after 24 h (if applicable) and investigated after 48 h.

RNF4-FLAG Purification—Parental MCF7 cells and MCF7 cells stably expressing RNF4-FLAG were grown in regular DMEM until confluent in ten 15-cm dishes (~0.2 billion cells). Cells were washed 3 times in ice-cold PBS before the addition of 3 ml of ice-cold lysis buffer to each plate (150 mM NaCl, 50 mM Tris, 0.5% sodium deoxycholate, 1.0% NP-40, buffered at pH 7.5, with every 10 ml of lysis buffer supplemented by 1 tablet of protease inhibitors + EDTA (Roche Applied Science)). Subsequently, cells were scraped in the lysis buffer on ice and collected in 50-ml tubes. The lysates were sonicated on ice for 10 s using a microtip sonicator at 30 watts. Next, lysates were centrifuged at 4 °C and 10,000 relative centrifugal force to clear debris from the soluble fraction. Lysates were equalized using the bicinchoninic acid assay (Pierce). 1 μl (dry volume) of FLAG-M2-agarose beads (Sigma) was prepared per 1 ml of lysate and equilibrated by washing 5 times in ice-cold lysis buffer. FLAG-M2 beads were added to the lysates and incubated while tumbling for 2 h at 4 °C. Next, beads were pelleted by centrifugation at 250 relative centrifugal force and washed 5 times with ice-cold lysis buffer. After every single wash step, the tubes were exchanged. RNF4-FLAG and interacting proteins were eluted off the beads by incubating them for 10 min with three bead volumes of lysis buffer supplemented with 1 mM FLAG-M2 peptide. Elution of the beads was repeated twice, and a fourth elution was performed with 2× LDS sample buffer (Novex). The primary three peptide elutions were pooled and concentrated. Culturing of cells, immunoprecipitation of RNF4-FLAG, and subsequent steps leading to the LC-MS/MS analysis were performed in biological triplicate.

Purification of His-SUMO-2—Purification of His-SUMO-2-modified proteins was essentially performed as described previously (8, 38).

Recombinant Proteins—His_6-MBP-USP11 and His-ΔN11-SUMO-2-Tetramer recombinant proteins were purified essentially as described previously (39). Briefly, BL21 cells were

transformed with expression constructs. Cells were grown to an A_{600} of 0.6. Subsequently, cells were grown overnight at 24 °C in the presence of 0.1 mM isopropyl-β-D-thiogalactopyranoside, 20 mM HEPES, pH 7.5, 1 mM $MgCl_2$, and 0.05% glucose. Lysates were prepared, and proteins were affinity-purified on TALON beads (BD Biosciences). GST-tagged RNF4 was produced in *Escherichia coli* and purified as described previously (11).

In Vitro Ubiquitination, Binding, and Deubiquitination Assays—15 ng of His-ΔN11-SUMO-2-Tetramer was *in vitro* ubiquitinated using 8 μM ubiquitin, 40 nM UBE1, 0.7 μM UbcH5a (all from Boston Biochem), 0.5 μM GST-RNF4 in 50 mM Tris, pH 7.5, 5 mM $MgCl_2$, 1 mM DTT, and 4 mM ATP. 50-μl reactions were incubated at 37 °C for 3 h after which non-ubiquitinated and ubiquitinated His-ΔN11-SUMO-2-Tetramers were bound to 50 μl of nickel-nitrilotriacetic acid beads, incubated for 3 h, and washed 4 times in washing buffer (50 mM Tris, pH 7.5, 150 mM NaCl, 25 mM $MgCl_2$, 20% glycerol, 0.1% Nonidet P-40, and 50 mM imidazole) before being eluted in washing buffer supplemented with 500 mM imidazole.

For the USP11 binding assay, purified non-ubiquitinated and ubiquitinated His-ΔN11-SUMO-2-Tetramers were incubated in the absence or presence of 5 μg of His_6-MBP-USP11 for 2 h at 4 °C. Subsequently, His_6-MBP-USP11 was purified through the addition of 25 μl of prewashed Amylose Resin (New England Biolabs). His_6-MBP-USP11 and amylose resin were incubated in EBC buffer (50 mM Tris, pH 7.5, 150 mM NaCl, 1 mM EDTA, 1 mM DTT, 0.5% Nonidet P-40) for 2 h at 4 °C, washed 5 times with EBC buffer, and eluted in 25 μl of 2× LDS sample buffer.

For the USP11 activity assay, purified ubiquitinated His-ΔN11-SUMO-2-Tetramers were incubated in 50 mM Tris, pH 7.5, 5 mM $MgCl_2$, and 2 mM DTT with different amounts (1–5 μg) of His_6-MBP-USP11 wild-type and catalytic-dead (C318A) proteins in a final volume of 20 μl. Reactions were incubated at 4 °C for 3 h. Reactions were stopped by the addition of 5 μl of 4× LDS sample buffer (Novex).

Antibodies—The following antibodies were used in this study: mouse α-FLAG (M2, Sigma), mouse α-PML (5E10, kind gift from Prof. R. van Driel, University of Amsterdam, The Netherlands (40)), rabbit α-USP11 (A301–613A, Bethyl), mouse α-SUMO-2/3 (8A2, Abcam), rabbit α-SUMO-2/3 (41), rabbit α-RNF4 (32), rabbit α-SART1 (41, 42), and rabbit α-V5 (V8137, Sigma).

Electrophoresis, Coomassie Staining, and In-gel Digestion—RNF4-FLAG immunoprecipitation (IP) samples were size-separated by SDS-PAGE using Novex 4–12% gradient gels and MES SDS running buffer (Life Technologies) followed by staining with a Colloidal Blue kit (Life Technologies). Gel lanes were excised as 10 slices per eluted fraction, cut into 2-mm^3 cubes, and in-gel digested with sequencing-grade-modified trypsin (Promega) as described before (43). The peptides extracted from the gel after digestion were cleaned, desalted, and concentrated on C18 reverse phase StageTips (44).

Electrophoresis and Immunoblotting—Samples were size-separated by SDS-PAGE using Novex 4–12% Bis-Tris gradient gels and MOPS SDS running buffer (Life Technologies) or homemade 8% acrylamide gels and Tris-glycine running buffer. Subsequently, proteins were transferred to nitrocellulose membranes (Amersham Biosciences) using a submarine system (Life Technologies). Sharp Pre-stained Protein Standard (Novex) was used as a size indicator for Fig. 1, and SeeBlue® Plus2 Protein Standard (Life Technologies) was used as a size indicator for Figs. 2–6. Note that SeeBlue® Plus2 migrates differently depending on the buffer conditions used, as documented on the manufacturer's website. Ponceau S staining and immunostaining were performed as described previously (38).

LC-MS/MS Analysis and Data Processing—Experiments were performed in triplicate. The analysis of in-gel-digested samples was performed as described previously (45). Raw data were processed using MaxQuant (46, 47). RNF4-FLAG interactors were investigated through label-free quantification as well as MS/MS spectral counting.

Microscopy—Cells were seeded on glass coverslips and fixed 24 h later for 10 min in 3.7% paraformaldehyde in PHEM buffer (60 mM PIPES, 25 mM HEPES, 10 mM EGTA, 2 mM $MgCl_2$, pH 6.9) at 37 °C. After washing with PBS, cells were permeated with 0.1% Triton X-100 for 10 min, washed with PBS-Tween (PBST), and blocked using TNB (100 mM Tris, pH 7.5, 150 mM NaCl, 0.5% Blocking Reagent (Roche Applied Science)) for 30 min. Cells were incubated with primary antibody as indicated in TNB for 1 h. Cells were washed 5 times with PBST and incubated with secondary antibodies (goat α-Ms Alexa 488 and goat α-Rb Alexa 594 (Life Technologies)) in TNB for 1 h. Next, cells were washed 5 times with PBST and dehydrated using alcohol before fixing them in DAPI solution (Citifluor). Images were recorded on a Leica SP5 confocal microscope system using 488- and 561-nm lasers for excitation and a 63× lens for magnification and were analyzed with Leica confocal software. For quantification of PML bodies, groups of cells were recorded in similar-sized fields using Z-stacking with steps of 0.5 μm to acquire 10 images ranging from the bottom to the top of the cells. Images were maximum-projected, individual cells were localized, and PML bodies were counted using in-house customized Stacks software (48).

Results

Purification of FLAG-tagged RNF4 from MCF7 Cells—SUMO-targeted ubiquitin ligase RNF4 specifically recognizes targets that are modified by multiple SUMOs through its SUMOylation interacting motifs (SIMs) (15, 49). Subsequently, these SUMOylated targets are ubiquitinated by RNF4, which can lead to the degradation of these proteins by the proteasome (26, 50, 51). Poly-SUMOylated targets of RNF4 have been identified employing a trap consisting of the RNF4 SIM domain (52).

We were interested in identifying SIM-independent RNF4 interactors. To facilitate this study, an MCF7 cell line stably expressing C-terminally FLAG-tagged RNF4 was generated (Fig. 1*A*). RNF4-FLAG was located correctly and exclusively in the nucleus (Fig. 1*B*). Some of the RNF4-FLAG localized into nuclear bodies, which likely correspond to PML nuclear bodies. The non-fused and co-expressing green fluorescent protein (GFP) was included as a control.

We performed FLAG IP and found that RNF4-FLAG is very efficiently purified (Fig. 1, *C* and *D*). Finally, Coomassie analysis

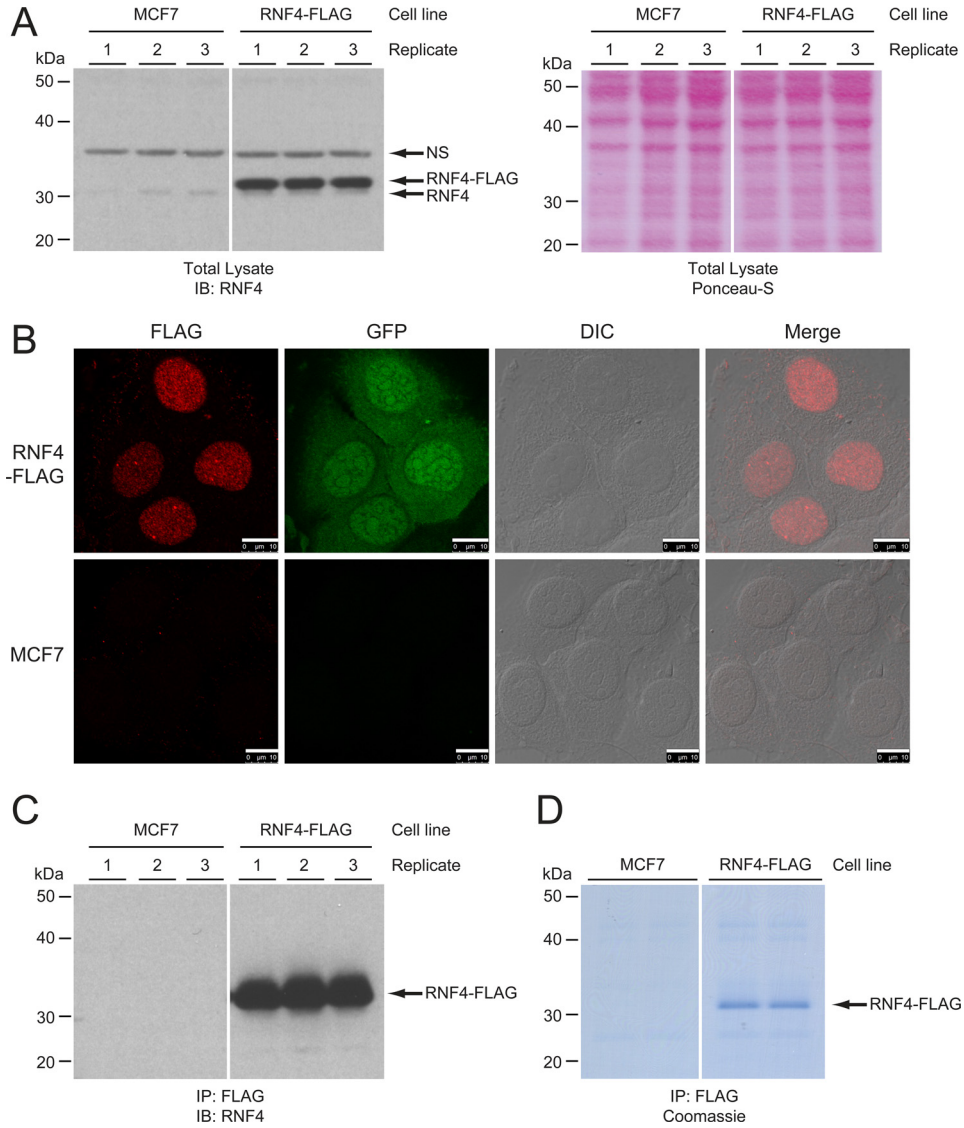

FIGURE 1. **Generation of a cell line stably expressing RNF4-FLAG.** *A*, MCF7 cells were infected with a bicistronic lentivirus encoding RNF4-FLAG and GFP separated by an internal ribosome entry site. Cells stably expressing low levels of the transgene were selected by flow cytometry. Total cell lysates were analyzed by immunoblotting to confirm expression of RNF4-FLAG. Ponceau S staining of the membrane was included as a loading control. The experiment was performed in biological triplicate for mass spectrometric analysis. *IB*, immunoblot. *NS*, nonspecific. *B*, stable cell lines were investigated by confocal fluorescent microscopy to confirm the nuclear localization of RNF4-FLAG. GFP was visualized as an expression control, and differential interference contrast (*DIC*) was used to visualize the nuclei. *Scale bars* are 10 μm. *C*, RNF4 complexes were purified by IP, and three biological replicates were analyzed by immunoblotting for the presence of RNF4. Parental cells were included as a negative control. *D*, Coomassie analysis of one replicate of the FLAG-IP, loaded over two lanes, before in-gel digestion and analysis by LC-MS/MS.

of the purified RNF4-FLAG and its potential interactors revealed a singular and very clear band corresponding to RNF4-FLAG, indicative of a clean and highly stringent purification of RNF4-FLAG (Fig. 1*D*).

Identification of Ubiquitin-specific Protease 11 (USP11) Co-purifying with RNF4—The RNF4-FLAG IP was performed in biological triplicate, and the gel lanes were cut in five separate slices and analyzed by mass spectrometry. Strikingly, we did not detect free or conjugated forms of SUMO in the IP, proving that our lysis and IP conditions were sufficiently harsh to yield a clean IP yet mild enough to allow the highly robust SUMO proteases to cleave SUMO off virtually all proteins. Unsurprisingly, RNF4 itself was detected as the highest enriched protein after RNF4-FLAG IP. Interestingly, we identified USP11 as an RNF4 interactor (Fig. 2*A*). USP11 was found to be enriched over the control with a $\log_2$ ratio of 5.1, and 11 MS/MS spectral identifications matching USP11 were made in the RNF4-FLAG IP as opposed to zero in the control IP (Fig. 2*A* and supplemental Table S1).

After identifying USP11 as a putative interactor of RNF4 through mass spectrometry analysis, the experiment was repeated, and samples were analyzed by immunoblotting (Fig. 2*B*). Additionally, a potential effect of the DNA damaging agent MMS on the interaction between RNF4 and USP11 was investigated, as MMS is known to cause disassembly of the nuclear bodies harboring RNF4 (53). After RNF4-FLAG IP, we found that endogenous USP11 interacted specifically with RNF4, with no signal detectable in the control (Fig. 2*B*). There was no indication that the interaction between RNF4 and USP11 is disrupted upon treating the cells with MMS. A small decrease in USP11 levels was observed after DNA damage, indicative of its

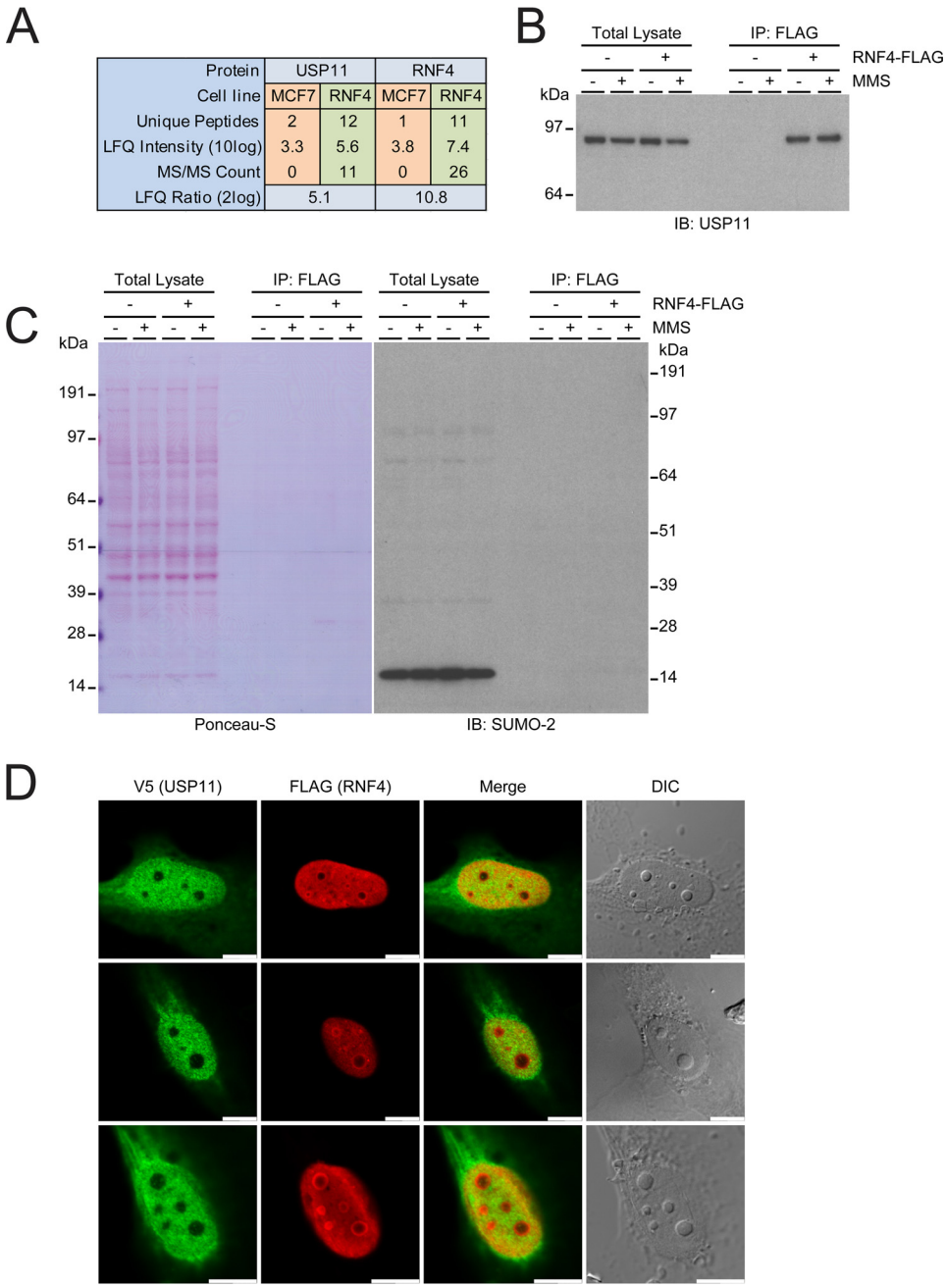

FIGURE 2. **Identification of USP11 as an RNF4-interacting ubiquitin protease.** *A*, overview of the mass spectrometry results pertaining to USP11 and RNF4. USP11 was found to be significantly enriched after FLAG-IP from the RNF4-FLAG stable cell line, with 0/0/0 USP11 MS/MS counts in the parental line *versus* 8/14/11 USP11 MS/MS counts in the RNF4-FLAG line, respectively. USP11 was found to be enriched after RNF4-FLAG IP with a label-free quantification (*LFQ*) $\log_2$ ratio of >5. *B*, MCF7 cell lines expressing RNF4-FLAG and parental controls were treated with MMS and lysed, and FLAG-IP was performed. Total lysates and IP fractions were analyzed by immunoblotting (*IB*) against USP11 to confirm the co-immunoprecipitation of endogenous USP11 with RNF4-FLAG. *C*, Ponceau S loading control for section B. Additionally, total lysates and IP fractions were analyzed by immunoblotting against SUMO-2/3 to investigate potential co-immunoprecipitation of SUMO-2/3 with RNF4 through its SIMs. *D*, investigation of V5-USP11 and FLAG-RNF4 co-localization. Both proteins were transiently expressed in U2-OS cells before the cells being fixed, immunostained, and analyzed by confocal fluorescence microscopy. Differential interference contrast (*DIC*) was used to visualize the nuclei and nucleoli. *Scale bars* represent 10 μm.

function in the DNA damage response. In agreement with the mass spectrometry findings, free SUMO was detected only in the total lysates, a direct result of the SUMO proteases removing all SUMO from target proteins after lysis, indicating that the interaction between USP11 and RNF4 is SUMOylation-independent (Fig. 2*C*). Finally, we investigated co-localization of USP11 and RNF4 through confocal microscopy. Whereas RNF4 was observed to be exclusively nuclear and USP11 was localized all throughout the cell, both proteins had a significant presence in the nucleus but outside of the nucleoli. This suggests that a fraction of these proteins resides in close proximity to each other in the nucleus (Fig. 2*D*).

USP11 Deubiquitinates SUMO-2-ubiquitin Hybrid Chains in Vitro—To test whether USP11 (Fig. 3*A*) can counteract RNF4 *in vitro*, a hybrid SUMO-2-ubiquitin polymer was generated as a potential USP11 substrate using a recombinant linear SUMO-2

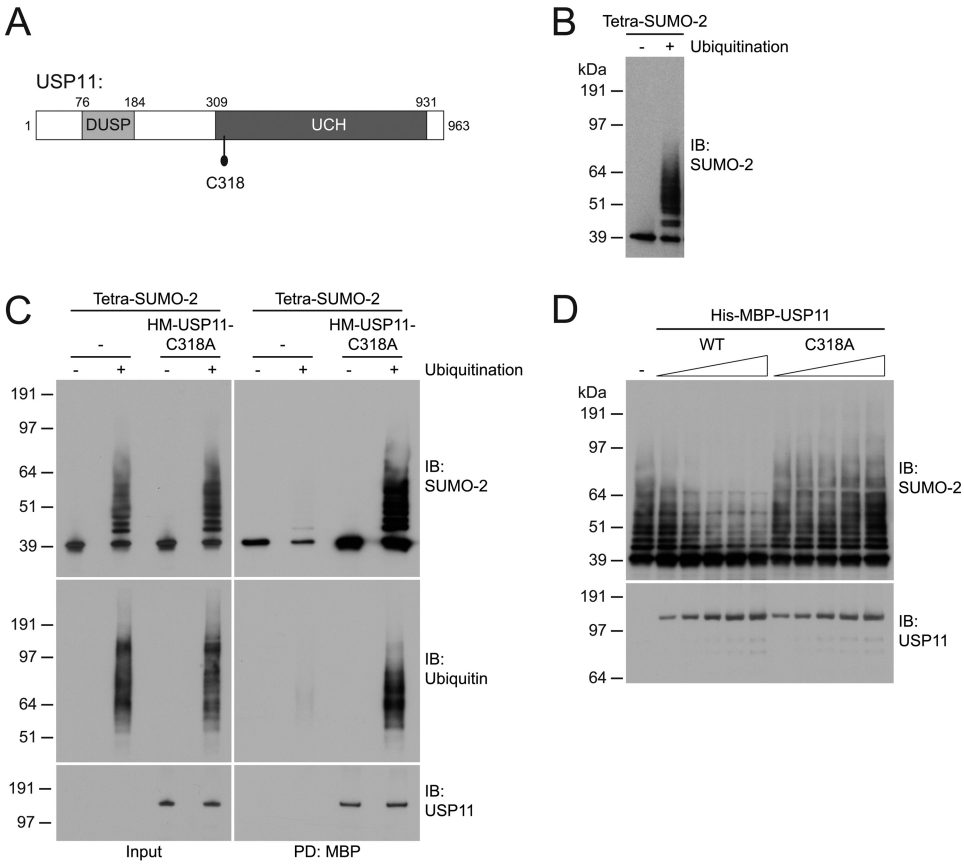

FIGURE 3. **USP11 deubiquitinates hybrid SUMO-2-ubiquitin chains *in vitro*.** *A*, schematic depiction of USP11. USP11 harbors a domain present in ubiquitin-specific proteases (DUSP) and a ubiquitin C-terminal hydrolase domain (*UCH*). The location of the catalytic cysteine (Cys-318) is indicated. *B*, His-tetra-SUMO-2 proteins were *in vitro* ubiquitinated using GST-RNF4. *IB*, immunoblot. *C*, His-tetra-SUMO-2 and hybrid SUMO-ubiquitin chains were incubated in the absence or presence of catalytic inactive His_6-MBP-USP11, before enrichment of His_6-MBP-USP11 by MBP pulldown (*PD*). Input and pulldown samples were analyzed by immunoblotting for SUMO-2/3 and ubiquitin, and input levels and pulldown efficiency were analyzed by immunoblotting for USP11. *D*, hybrid SUMO-ubiquitin chains were incubated with increasing concentrations of His_6-MBP-USP11 wild-type (*WT*) or a catalytic inactive mutant (C318A). Hybrid chains were analyzed by immunoblotting against SUMO-2/3, and His_6-MBP-USP11 input levels were analyzed by immunoblotting for USP11.

polymer composed of four SUMO moieties that was ubiquitinated *in vitro* by RNF4 (Fig. 3*B*) (26). We investigated the ability of a catalytically inactive USP11 mutant (C318A) to bind to hybrid SUMO-2-ubiquitin chains through a binding assay, and USP11 was observed to bind to these hybrid chains with very high efficiency regardless of whether singular or multiple ubiquitin moieties were coupled to the tetra-SUMO-2 (Fig. 3*C*). Next, we performed a deubiquitination assay and observed that wild-type USP11 was able to deubiquitinate SUMO-2-ubiquitin hybrid chains, whereas the catalytically inactive USP11 mutant had no effect (Fig. 3*D*). We conclude that USP11 could efficiently bind to and deubiquitinate hybrid SUMO-2-ubiquitin polymers generated by RNF4 *in vitro*.

USP11 Counterbalances RNF4 and Controls Stability of Nuclear Bodies—Because RNF4 is known to ubiquitinate SUMOylated PML, which in turn leads to degradation of PML and the destabilization of nuclear bodies (26), we set out to study the role of endogenous USP11 in nuclear body integrity. Lentiviral shRNA-mediated depletion of endogenous USP11, RNF4, or both proteins was performed before analysis of the cells by confocal microscopy (Fig. 4*A*). Although SUMO and PML co-localize in nuclear bodies, the overlap is partial. Strikingly, after depletion of endogenous USP11, a significant reduction in nuclear bodies was observed (Fig. 4*A*). Accordingly, depletion of endogenous RNF4 led to significant increases in nuclear bodies. Ultimately, an ~25% reduction in PML bodies and an ~50% reduction in SUMO bodies was found upon USP11 depletion, and an ~35% increase in PML bodies and an ~50% increase in SUMO bodies was found upon RNF4 depletion (Fig. 4*B*). Efficient depletion of both USP11 and RNF4 was confirmed (Fig. 4*C*). Similar results were obtained in MCF7 cells (data not shown).

Interestingly, when combining depletion of both USP11 and RNF4, a somewhat intermediate phenotype was observed (Fig. 4, *A* and *B*). Whereas the increase in PML bodies resulting from depletion of RNF4 was modestly countered by additional knockdown of USP11, there was no clear effect on SUMO-positive nuclear bodies. Thus, it is likely that USP11 acts downstream of RNF4, providing a counterbalancing mechanism to the ubiquitin ligase activity of RNF4 to establish an important equilibrium, which is characteristic for ubiquitin signaling and a general phenomenon for post-translational modifications.

USP11 Modulates the Level of SUMOylated PML—In addition to cellular analysis by microcopy, the SUMOylation state of the PML protein after depletion of endogenous USP11 in HeLa cells was investigated. To facilitate the experiment, HeLa cell

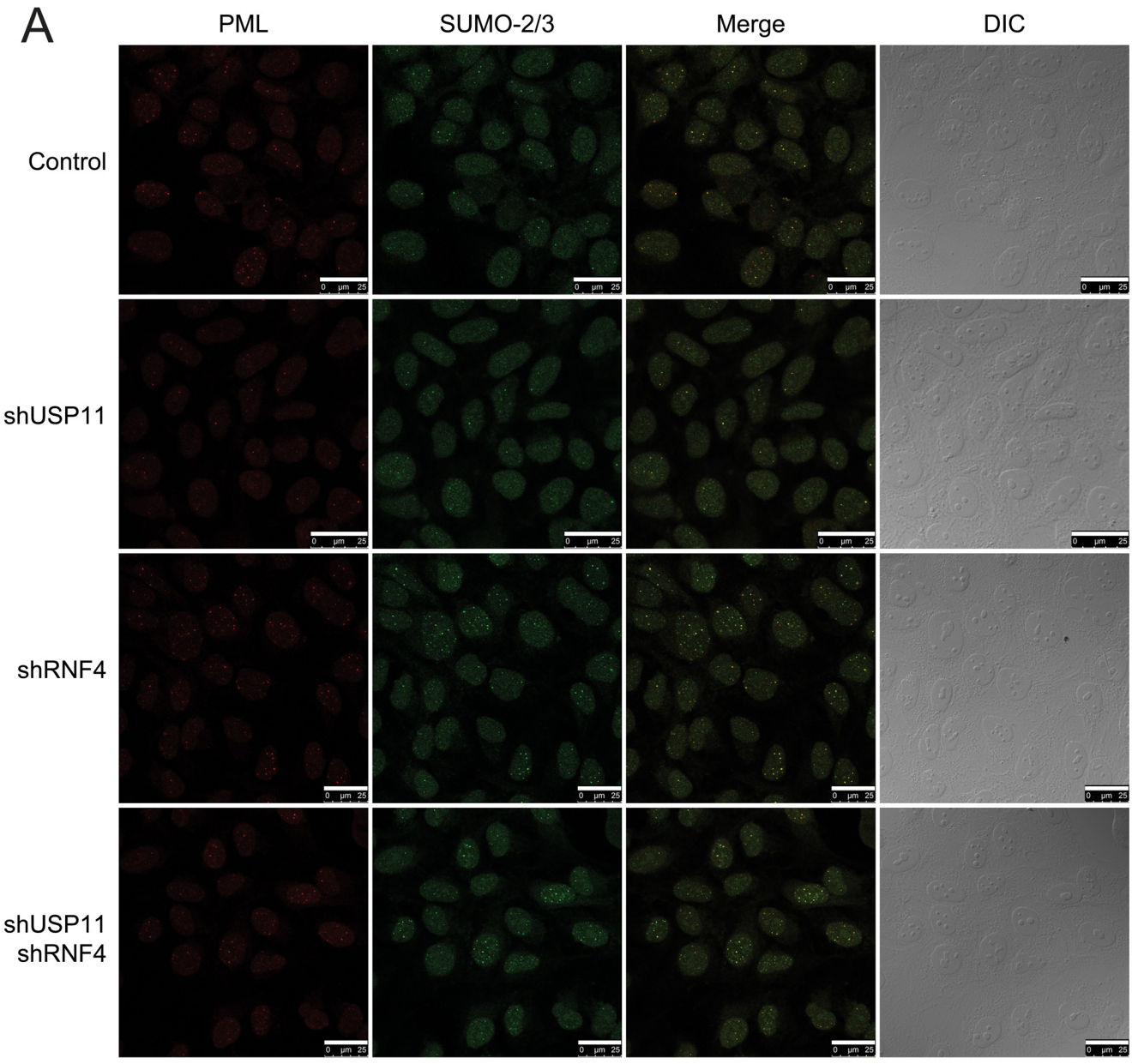
A
PML
SUMO-2/3
Merge
DIC
Control
shUSP11
shRNF4
shUSP11
shRNF4

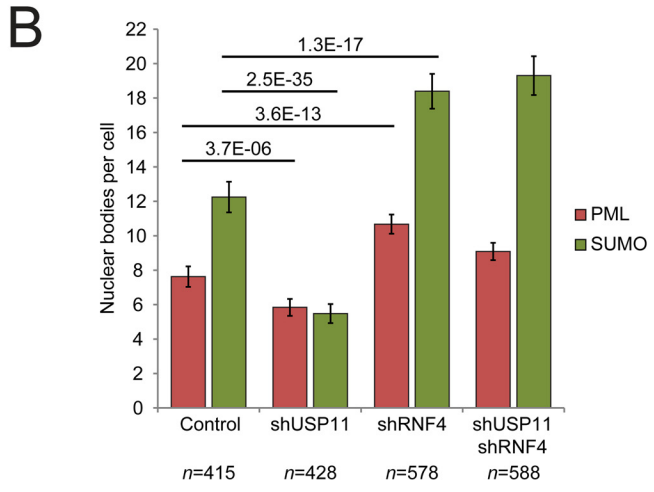
B
Nuclear bodies per cell
22
20
18
16
14
12
10
8
6
4
2
0
1.3E-17
2.5E-35
3.6E-13
3.7E-06
PML
SUMO
Control
shUSP11
shRNF4
shUSP11
shRNF4
n=415
n=428
n=578
n=588

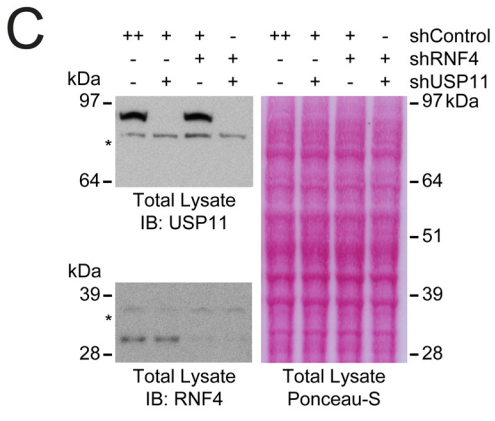
C
++ + + - ++ + + - shControl
- - + + - - + + shRNF4
kDa - + - + - + - + shUSP11
97
64
Total Lysate
IB: USP11
kDa
39
28
Total Lysate
IB: RNF4
Total Lysate
Ponceau-S
97 kDa
64
51
39
28

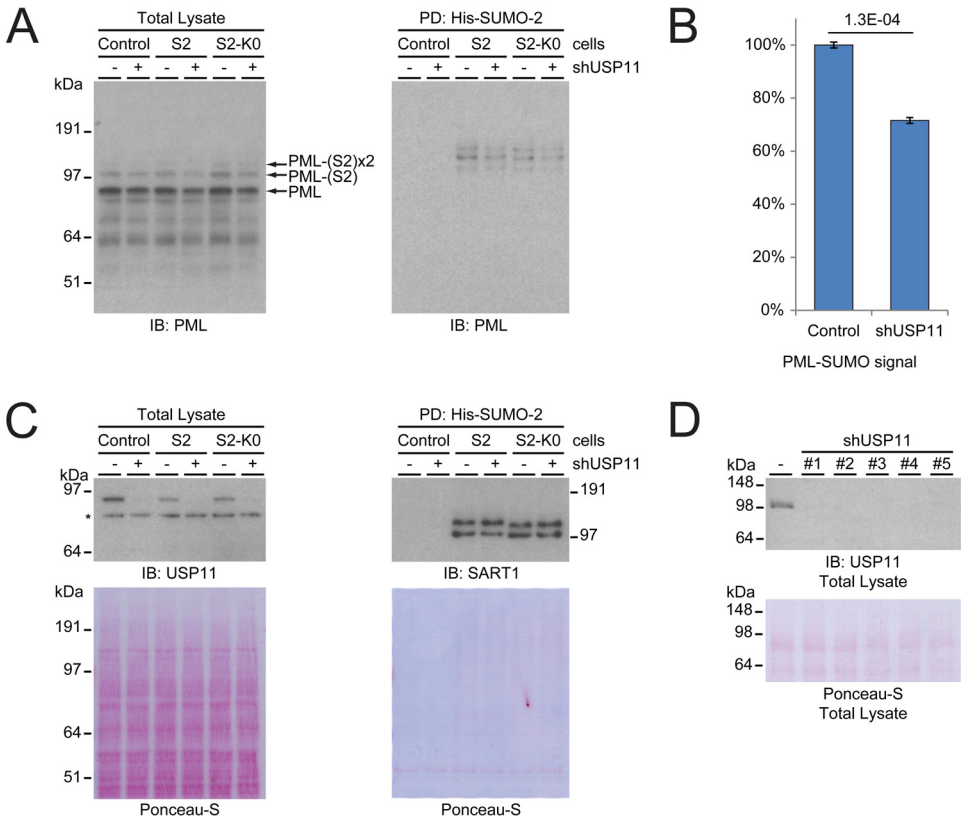

FIGURE 5. **USP11 stabilizes SUMOylated PML.** *A*, HeLa cells expressing wild-type His-tagged SUMO-2 or lysine-deficient SUMO-2 and parental HeLa cells were either depleted for USP11 by infection with lentiviral knockdown constructs or treated with an untargeted knockdown construct. After depletion of USP11, cells were lysed, and His pulldown (*PD*) was performed to enrich SUMOylated proteins. Total lysates and SUMO-enriched fractions were analyzed by immunoblotting (*IB*) using an antibody against PML. Unmodified and SUMO-modified PML are indicated for the total lysate blot. *B*, quantification of the PML-SUMO signal in the total lysate and SUMO-enriched lanes corresponding to the His-SUMO cell lines, comparing the PML-SUMO signal in the control *versus* USP11-depleted cells. *Error bars* represent S.D. Student's *t* test *p* value is indicated. *C*, total lysates from *A* were analyzed by immunoblotting with an antibody against USP11 as a knockdown control, and Ponceau S staining was used as a loading control. SUMO-enriched fractions from *A* were analyzed by immunoblotting with an antibody against SART1 as a SUMO-level control, and Ponceau S staining was used as a pulldown control. Note that SART1 modified with lysine-deficient SUMO has slightly different migration behavior due to lysine-to-arginine substitutions. *D*, HeLa cells were depleted of USP11 by infection with five different lentiviral knockdown constructs or treated with an untargeted knockdown construct. Subsequently, cells were lysed, and total lysates were analyzed by immunoblotting using an antibody against USP11. All five viruses were found to be efficient, and a low concentration mixture of all viruses was used for all other USP11 depletion experiments to provide an effective knockdown. Note that this experiment was performed using an acrylamide gel resolved in Tris-glycine buffer, which accounts for a slightly different observed migration size of USP11.

lines stably expressing His-tagged SUMO-2 were used to allow for efficient purification of SUMOylated proteins. Additionally, a similar cell line stably expressing lysine-deficient His-tagged SUMO-2 was used to investigate a potential effect of inhibited SUMO-2 chain formation on the SUMOylation of PML and any cumulative result in combination with USP11 depletion.

Similar to observations made with counting PML bodies, a significant decrease in SUMOylated PML was found after depletion of USP11 in both total lysate and SUMO-enriched fractions (Fig. 5*A*). We noted a very slight decrease in total PML levels after USP11 depletion, which could be a direct result of SUMOylated and subsequently ubiquitinated PML being degraded more rapidly. The decrease in SUMOylated PML signal was found to be ~30% (Fig. 5*B*), highly similar to the ~25% decrease in PML nuclear bodies observed through confocal microscopy (Fig. 4*B*). We observed a somewhat lower SUMOylation efficiency of PML modification by lysine-deficient SUMO. However, USP11 depletion still resulted in a consistent decrease of PML SUMOylation. Efficient depletion of endogenous USP11 was validated (Fig. 5, *C* and *D*), and additionally the well known SUMOylation target protein SART1 (39) was investigated as a control (Fig. 5*C*). The SUMOylation state of SART1 was virtually identical regardless of USP11 depletion, indicating that the effect on PML SUMOylation was specific. Note that the slight shift in

FIGURE 4. **USP11 stabilizes nuclear bodies, counteracting the destabilizing effect of RNF4.** *A*, U2-OS cells were depleted for endogenous USP11, RNF4, or both by infection with lentiviral knockdown constructs. As a control, an untargeted lentiviral knockdown construct was used. After depletion of proteins, cells were fixed, immunostained, and subsequently analyzed by confocal fluorescence microscopy for the presence of PML- and SUMO-2/3-positive nuclear bodies. Images represent maximum projections of Z-stacks. Differential interference contrast (*DIC*) was used to visualize the nuclei. Depletion of USP11 destabilizes PML and SUMO-2/3 nuclear bodies, whereas depletion of RNF4 stabilizes PML and SUMO-2/3 nuclear bodies. *Scale bars* are 25 μm. *B*, multiple maximum projected fields of cells were recorded as in *A*. Cells were counted, and PML and SUMO-2/3 nuclear bodies were quantified per cell. At least 400 cells were counted for each experimental condition, with the exact number of cells shown *below each experiment*. *Error bars* represent 2× S.E. Student's *t* test *p* values are indicated *over their respective experiments*. *C*, total cell lysates were analyzed by immunoblotting (*IB*) to confirm the depletion of USP11 and RNF4. Ponceau S staining of the membrane was included as a loading control.

migration behavior visible between the wild-type SUMO-2 and the lysine-deficient SUMO-2 is a direct effect of lysine-to-arginine substitutions.

USP11 Prevents the Disintegration of Nuclear Bodies in Response to DNA Damage—To investigate the extent of protection USP11 offers to SUMOylated PML and their associated

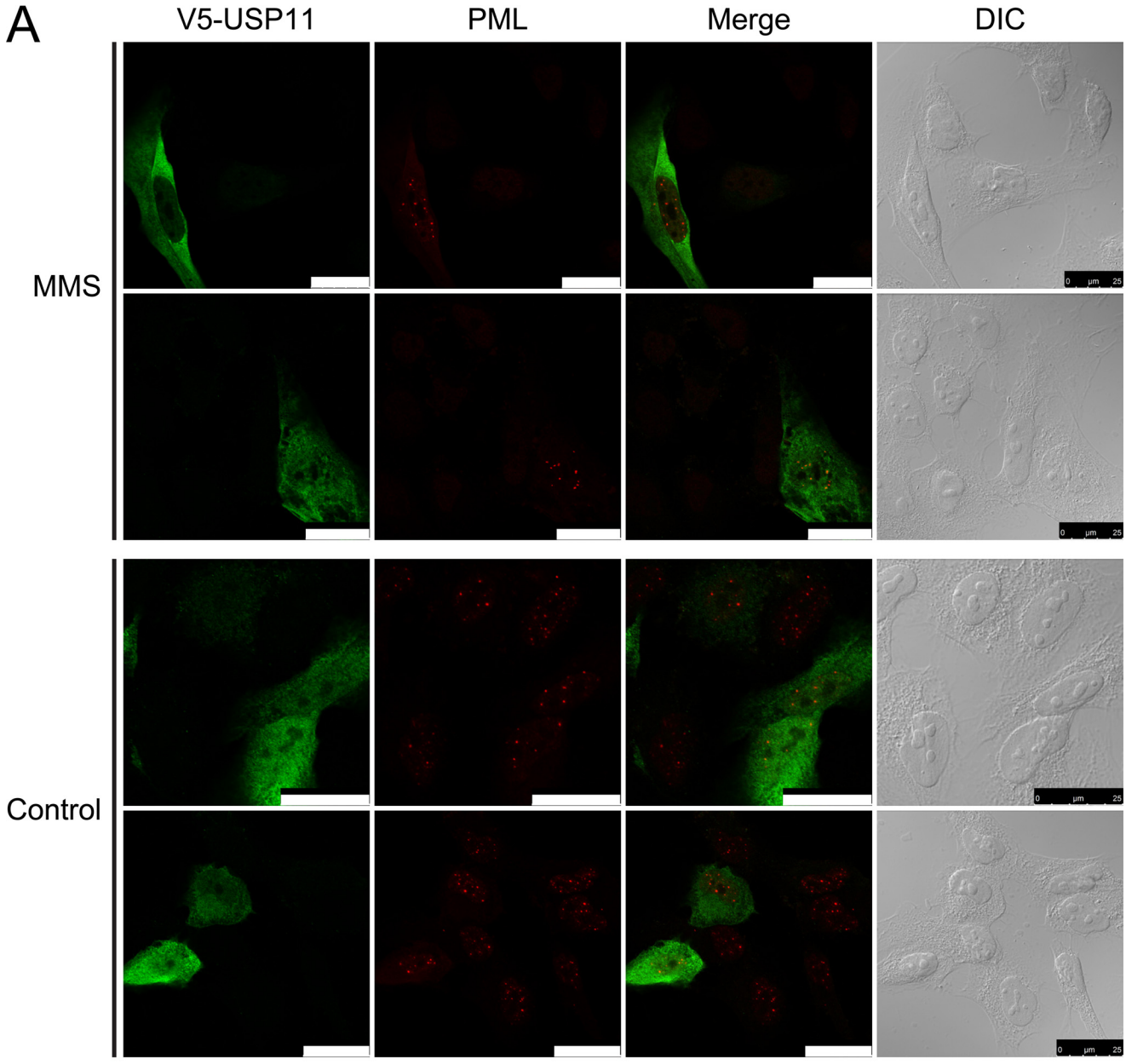

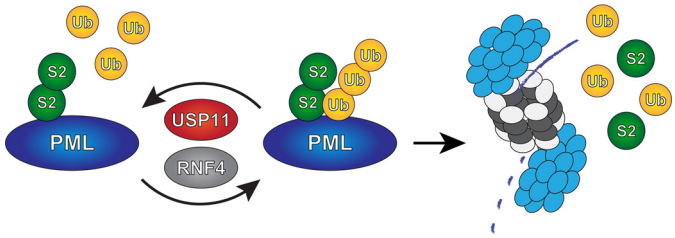

FIGURE 7. **Model.** USP11 counteracts RNF4 by deubiquitinating SUMO-ubiquitin hybrid chains generated by RNF4, preventing degradation of PML by the proteasome.

nuclear bodies, an overexpression experiment was performed where U2-OS cells were transfected with V5-tagged USP11. Subsequently, the cells were treated with MMS, which is known to cause degradation of SUMOylated PML and instigate a disassembly of nuclear bodies (53–55). The treatment dose and time chosen for the experiment was sufficient to completely abolish all PML nuclear bodies. Confocal fluorescence microscopy was used to investigate mock-treated and MMS-treated cells (Fig. 6*A*).

In untreated cells, nuclear bodies were observed to be distributed fairly equally between cells expressing V5-USP11 and untransfected cells. However, after MMS treatment virtually all untransfected cells completely lost their nuclear bodies, whereas some cells expressing V5-USP11 were able to retain their PML bodies (Fig. 6*A*). We quantified >100 cells that retained PML bodies and found the large majority (~92%) to express V5-USP11 even though only ~28% of all cells were transfected (Fig. 6*B*). Equal expression of V5-USP11 was confirmed by immunoblotting (Fig. 6*C*). Thus, an increased presence of USP11 within the cell was able to counteract the ubiquitination and degradation of SUMOylated PML and could counteract the disassembly of nuclear bodies in response to DNA damage (Fig. 7).

Discussion

Using an unbiased proteomic approach, we have identified USP11 as a ubiquitin protease to co-purify with RNF4, with the ability to process hybrid SUMO-ubiquitin polymers. This USP family member contains a DUSP domain with the ability to bind ubiquitin as well as a catalytic UCH domain. We found that USP11 was able to deubiquitinate hybrid SUMO-ubiquitin chains via its catalytically active C-terminal hydrolase domain. Furthermore, USP11 possessed the ability to counteract RNF4 during regular growth conditions. Depletion of USP11 led to a decrease in the amount of nuclear bodies, whereas depletion of RNF4 led to the exact opposite. Furthermore, we found that exogenous USP11 could counteract the role of RNF4 in the DNA damage response by blocking the dissociation of PML bodies in response to MMS. The dissociation of PML bodies enables proper progression of the DNA damage response (56) and induction of apoptosis (57, 58).

USP11 was previously found to be involved in repair of double-stranded breaks by homologous recombination, where knockdown of USP11 resulted in spontaneous activation of DNA damage response pathways, rendering cells hypersensitive to poly(ADP-ribose) polymerase inhibition, ionizing radiation and other genotoxic stresses (59). USP11 has been shown to interact with BRCA2, a key component of the homologous recombination pathway, where BRCA2 was shown to be a target for deubiquitination by USP11 (60). Treatment of cells by mitomycin C led to degradation of BRCA2, which could be countered by USP11 overexpression, and inhibition of USP11 function increased cellular sensitivity to mitomycin C (60). Similar to USP11, RNF4 is also required for homologous recombination (30–32), indicating that balanced ubiquitination and deubiquitination of SUMOylated proteins is required for efficient DNA repair via homologous recombination.

The function of USP11 in the DNA damage response makes it a potential clinical target, as inhibition of USP11 would render cancer cells susceptible to apoptosis, especially combined with other treatments such as poly(ADP-ribose) polymerase inhibition. Accordingly, some progress has been made on compounds targeting and counteracting USP11, displaying the ability to inhibit growth of pancreatic cancer cells (61).

In a similar screen for interaction partners of varying deubiquitinating enzymes performed by Sowa *et al.* (62), RNF4 was not discovered as an interaction partner of USP11. However, different buffer conditions, epitope tags, and cell lines were used, which could account for variations in interactomes between the two screens.

More recently, USP11 was found to interact directly with PML (63). Contrarily, we found USP11 to co-purify with the SUMO-targeted ubiquitin ligase RNF4. Wu *et al.* (63) further reported that USP11 depletion leads to a decrease in PML bodies, which is consistent with our findings. USP11 overexpression was shown by Wu *et al.* (63) to be able to counteract arsenic-induced degradation of PML, but a role in the DNA damage response was not investigated by these authors. USP11 was found to be transcriptionally repressed in human glioma, with up-regulation of the Hey1/Notch pathway resulting in down-regulation of USP11 and correspondingly PML (63). Interestingly, this was found to increase cellular malignancy as well as potentiate survival and resistance to therapeutic treatment, which opposes findings where antagonizing USP11 leads to inhibition of pancreatic cancer (61).

In summary, we propose that USP11 keeps RNF4 in check through its ability to reverse RNF4 ubiquitination of SUMOylated proteins (Fig. 7). We have thus identified a ubiq-

FIGURE 6. **USP11 counteracts RNF4-mediated degradation of nuclear bodies in response to treatment with the DNA damaging agent methyl methanesulfonate.** *A*, U2-OS cells were transfected with a construct encoding V5-USP11 and subsequently mock-treated or treated with 0.02% MMS for 135 min. After treatment, cells were fixed and immunostained. Confocal fluorescence microscopy was used to visualize V5-USP11 (*green*) and PML (*red*). Differential interference contrast (*DIC*) was used to visualize the nuclei. *Scale bars* are 25 μm. *B*, as in *A*, except 143 cells that retained PML bodies after MMS treatment were investigated for the presence of V5-USP11. V5-USP11 transfection efficiency of all cells was 27.6%. The randomly expected number of cells expressing V5-USP11 retaining PML bodies was 39 (27.6%) *versus* the experimentally observed amount of 132 (92.3%). This difference was significant with a p value of 2.0E-185 by Pearson's χ^2 test. *C*, immunoblot (*IB*) analysis of total lysates corresponding to section A. V5 antibody was used to confirm exogenous expression of V5-USP11, and Ponceau S staining was used as a loading control.

uitin protease that balances the activity of a SUMO-targeted ubiquitin ligase.

Acknowledgments—We are grateful to Drs. R. van Driel, R. T. Hay, R. C. Hoeben, L. Fradkin, L. Zhong and P. ten Dijke for providing critical reagents, M. Verlaan-de Vries for technical assistance, and Dr. A. Zemla for providing artwork. The NNF Center for Protein Research is supported by a generous donation from the Novo Nordisk Foundation.

References

1. Flotho, A., and Melchior, F. (2013) Sumoylation: a regulatory protein modification in health and disease. *Annu. Rev. Biochem.* **82,** 357–385
2. Hickey, C. M., Wilson, N. R., and Hochstrasser, M. (2012) Function and regulation of SUMO proteases. *Nat. Rev. Mol. Cell Biol.* **13,** 755–766
3. Hay, R. T. (2007) SUMO-specific proteases: a twist in the tail. *Trends Cell Biol.* **17,** 370–376
4. Nacerddine, K., Lehembre, F., Bhaumik, M., Artus, J., Cohen-Tannoudji, M., Babinet, C., Pandolfi, P. P., and Dejean, A. (2005) The SUMO pathway is essential for nuclear integrity and chromosome segregation in mice. *Dev. Cell* **9,** 769–779
5. Becker, J., Barysch, S. V., Karaca, S., Dittner, C., Hsiao, H. H., Berriel Diaz, M., Herzig, S., Urlaub, H., and Melchior, F. (2013) Detecting endogenous SUMO targets in mammalian cells and tissues. *Nat. Struct. Mol. Biol.* **20,** 525–531
6. Golebiowski, F., Matic, I., Tatham, M. H., Cole, C., Yin, Y., Nakamura, A., Cox, J., Barton, G. J., Mann, M., and Hay, R. T. (2009) System-wide changes to SUMO modifications in response to heat shock. *Sci. Signal.* **2,** ra24
7. Vertegaal, A. C. (2011) Uncovering ubiquitin and ubiquitin-like signaling networks. *Chem. Rev.* **111,** 7923–7940
8. Matic, I., Schimmel, J., Hendriks, I. A., van Santen, M. A., van de Rijke, F., van Dam, H., Gnad, F., Mann, M., and Vertegaal, A. C. (2010) Site-specific identification of SUMO-2 targets in cells reveals an inverted SUMOylation motif and a hydrophobic cluster SUMOylation motif. *Mol. Cell* **39,** 641–652
9. Rodriguez, M. S., Dargemont, C., and Hay, R. T. (2001) SUMO-1 conjugation *in vivo* requires both a consensus modification motif and nuclear targeting. *J. Biol. Chem.* **276,** 12654–12659
10. Bernier-Villamor, V., Sampson, D. A., Matunis, M. J., and Lima, C. D. (2002) Structural basis for E2-mediated SUMO conjugation revealed by a complex between ubiquitin-conjugating enzyme Ubc9 and RanGAP1. *Cell* **108,** 345–356
11. Tatham, M. H., Jaffray, E., Vaughan, O. A., Desterro, J. M., Botting, C. H., Naismith, J. H., and Hay, R. T. (2001) Polymeric chains of SUMO-2 and SUMO-3 are conjugated to protein substrates by SAE1/SAE2 and Ubc9. *J. Biol. Chem.* **276,** 35368–35374
12. Matic, I., van Hagen, M., Schimmel, J., Macek, B., Ogg, S. C., Tatham, M. H., Hay, R. T., Lamond, A. I., Mann, M., and Vertegaal, A. C. (2008) *In vivo* identification of human small ubiquitin-like modifier polymerization sites by high accuracy mass spectrometry and an *in vitro* to *in vivo* strategy. *Mol. Cell Proteomics* **7,** 132–144
13. Vertegaal, A. C. (2007) Small ubiquitin-related modifiers in chains. *Biochem. Soc. Trans.* **35,** 1422–1423
14. Vertegaal, A. C. (2010) SUMO chains: polymeric signals. *Biochem. Soc. Trans.* **38,** 46–49
15. Kerscher, O. (2007) SUMO junction-what's your function? New insights through SUMO-interacting motifs. *EMBO Rep.* **8,** 550–555
16. Danielsen, J. R., Povlsen, L. K., Villumsen, B. H., Streicher, W., Nilsson, J., Wikström, M., Bekker-Jensen, S., and Mailand, N. (2012) DNA damage-inducible SUMOylation of HERC2 promotes RNF8 binding via a novel SUMO-binding Zinc finger. *J. Cell Biol.* **197,** 179–187
17. Hunter, T., and Sun, H. (2008) Crosstalk between the SUMO and ubiquitin pathways. *Ernst. Schering. Found. Symp. Proc.* **1,** 1–16
18. Ulrich, H. D. (2005) Mutual interactions between the SUMO and ubiquitin systems: a plea of no contest. *Trends Cell Biol.* **15,** 525–532
19. Desterro, J. M., Rodriguez, M. S., and Hay, R. T. (1998) SUMO-1 modification of IκBα inhibits NF-κB activation. *Mol. Cell* **2,** 233–239
20. Huang, T. T., Wuerzberger-Davis, S. M., Wu, Z. H., and Miyamoto, S. (2003) Sequential modification of NEMO/IKKgamma by SUMO-1 and ubiquitin mediates NF-κB activation by genotoxic stress. *Cell* **115,** 565–576
21. Schimmel, J., Larsen, K. M., Matic, I., van Hagen, M., Cox, J., Mann, M., Andersen, J. S., and Vertegaal, A. C. (2008) The ubiquitin-proteasome system is a key component of the SUMO-2/3 cycle. *Mol. Cell Proteomics* **7,** 2107–2122
22. Tatham, M. H., Matic, I., Mann, M., and Hay, R. T. (2011) Comparative proteomic analysis identifies a role for SUMO in protein quality control. *Sci. Signal.* **4,** rs4
23. Prudden, J., Pebernard, S., Raffa, G., Slavin, D. A., Perry, J. J., Tainer, J. A., McGowan, C. H., and Boddy, M. N. (2007) SUMO-targeted ubiquitin ligases in genome stability. *EMBO J.* **26,** 4089–4101
24. Sun, H., Leverson, J. D., and Hunter, T. (2007) Conserved function of RNF4 family proteins in eukaryotes: targeting a ubiquitin ligase to SUMOylated proteins. *EMBO J.* **26,** 4102–4112
25. Uzunova, K., Göttsche, K., Miteva, M., Weisshaar, S. R., Glanemann, C., Schnellhardt, M., Niessen, M., Scheel, H., Hofmann, K., Johnson, E. S., Praefcke, G. J., and Dohmen, R. J. (2007) Ubiquitin-dependent proteolytic control of SUMO conjugates. *J. Biol. Chem.* **282,** 34167–34175
26. Tatham, M. H., Geoffroy, M. C., Shen, L., Plechanovova, A., Hattersley, N., Jaffray, E. G., Palvimo, J. J., and Hay, R. T. (2008) RNF4 is a poly-SUMO-specific E3 ubiquitin ligase required for arsenic-induced PML degradation. *Nat. Cell Biol.* **10,** 538–546
27. Sun, H., and Hunter, T. (2012) Poly-small ubiquitin-like modifier (Poly-SUMO)-binding proteins identified through a string search. *J. Biol. Chem.* **287,** 42071–42083
28. Poulsen, S. L., Hansen, R. K., Wagner, S. A., van Cuijk, L., van Belle, G. J., Streicher, W., Wikström, M., Choudhary, C., Houtsmuller, A. B., Marteijn, J. A., Bekker-Jensen, S., and Mailand, N. (2013) RNF111/Arkadia is a SUMO-targeted ubiquitin ligase that facilitates the DNA damage response. *J. Cell Biol.* **201,** 797–807
29. Heideker, J., Perry, J. J., and Boddy, M. N. (2009) Genome stability roles of SUMO-targeted ubiquitin ligases. *DNA Repair* **8,** 517–524
30. Yin, Y., Seifert, A., Chua, J. S., Maure, J. F., Golebiowski, F., and Hay, R. T. (2012) SUMO-targeted ubiquitin E3 ligase RNF4 is required for the response of human cells to DNA damage. *Genes Dev.* **26,** 1196–1208
31. Galanty, Y., Belotserkovskaya, R., Coates, J., and Jackson, S. P. (2012) RNF4, a SUMO-targeted ubiquitin E3 ligase, promotes DNA double-strand break repair. *Genes Dev.* **26,** 1179–1195
32. Vyas, R., Kumar, R., Clermont, F., Helfricht, A., Kalev, P., Sotiropoulou, P., Hendriks, I. A., Radaelli, E., Hochepied, T., Blanpain, C., Sablina, A., van Attikum, H., Olsen, J. V., Jochemsen, A. G., Vertegaal, A. C., and Marine, J. C. (2013) RNF4 is required for DNA double-strand break repair *in vivo*. *Cell Death Differ.* **20,** 490–502
33. Luo, K., Zhang, H., Wang, L., Yuan, J., and Lou, Z. (2012) Sumoylation of MDC1 is important for proper DNA damage response. *EMBO J.* **31,** 3008–3019
34. van Hagen, M., Overmeer, R. M., Abolvardi, S. S., and Vertegaal, A. C. (2010) RNF4 and VHL regulate the proteasomal degradation of SUMO-conjugated hypoxia-inducible factor-2α. *Nucleic Acids Res.* **38,** 1922–1931
35. Hu, X. V., Rodrigues, T. M., Tao, H., Baker, R. K., Miraglia, L., Orth, A. P., Lyons, G. E., Schultz, P. G., and Wu, X. (2010) Identification of RING finger protein 4 (RNF4) as a modulator of DNA demethylation through a functional genomics screen. *Proc. Natl. Acad. Sci. U.S.A.* **107,** 15087–15092
36. Nijman, S. M., Luna-Vargas, M. P., Velds, A., Brummelkamp, T. R., Dirac, A. M., Sixma, T. K., and Bernards, R. (2005) A genomic and functional inventory of deubiquitinating enzymes. *Cell* **123,** 773–786
37. Reyes-Turcu, F. E., Ventii, K. H., and Wilkinson, K. D. (2009) Regulation and cellular roles of ubiquitin-specific deubiquitinating enzymes. *Annu. Rev. Biochem.* **78,** 363–397
38. Hendriks, I. A., D'Souza, R. C., Yang, B., Verlaan-de Vries, M., Mann, M.,

and Vertegaal, A. C. (2014) Uncovering global SUMOylation signaling networks in a site-specific manner. *Nat. Struct. Mol. Biol.* **21,** 927–936
39. Schimmel, J., Balog, C. I., Deelder, A. M., Drijfhout, J. W., Hensbergen, P. J., and Vertegaal, A. C. (2010) Positively charged amino acids flanking a sumoylation consensus tetramer on the 110-kDa tri-snRNP component SART1 enhance sumoylation efficiency. *J. Proteomics* **73,** 1523–1534
40. Stuurman, N., de Graaf, A., Floore, A., Josso, A., Humbel, B., de Jong, L., and van Driel, R. (1992) A monoclonal antibody recognizing nuclear matrix-associated nuclear bodies. *J. Cell Sci.* **101,** 773–784
41. Vertegaal, A. C., Ogg, S. C., Jaffray, E., Rodriguez, M. S., Hay, R. T., Andersen, J. S., Mann, M., and Lamond, A. I. (2004) A proteomic study of SUMO-2 target proteins. *J. Biol. Chem.* **279,** 33791–33798
42. Vertegaal, A. C., Andersen, J. S., Ogg, S. C., Hay, R. T., Mann, M., and Lamond, A. I. (2006) Distinct and overlapping sets of SUMO-1 and SUMO-2 target proteins revealed by quantitative proteomics. *Mol. Cell Proteomics* **5,** 2298–2310
43. Shevchenko, A., Tomas, H., Havlis, J., Olsen, J. V., and Mann, M. (2006) In-gel digestion for mass spectrometric characterization of proteins and proteomes. *Nat. Protoc.* **1,** 2856–2860
44. Rappsilber, J., Mann, M., and Ishihama, Y. (2007) Protocol for micro-purification, enrichment, pre-fractionation, and storage of peptides for proteomics using StageTips. *Nat. Protoc.* **2,** 1896–1906
45. Schimmel, J., Eifler, K., Sigurðsson, J. O., Cuijpers, S. A., Hendriks, I. A., Verlaan-de Vries, M., Kelstrup, C. D., Francavilla, C., Medema, R. H., Olsen, J. V., and Vertegaal, A. C. (2014) Uncovering SUMOylation dynamics during cell-cycle progression reveals FoxM1 as a key mitotic SUMO target protein. *Mol. Cell* **53,** 1053–1066
46. Cox, J., Neuhauser, N., Michalski, A., Scheltema, R. A., Olsen, J. V., and Mann, M. (2011) Andromeda: a peptide search engine integrated into the MaxQuant environment. *J. Proteome. Res.* **10,** 1794–1805
47. Cox, J., and Mann, M. (2008) MaxQuant enables high peptide identification rates, individualized p.p.b.-range mass accuracies and proteome-wide protein quantification. *Nat. Biotechnol.* **26,** 1367–1372
48. Smeenk, G., Wiegant, W. W., Vrolijk, H., Solari, A. P., Pastink, A., and van Attikum, H. (2010) The NuRD chromatin-remodeling complex regulates signaling and repair of DNA damage. *J. Cell Biol.* **190,** 741–749
49. Lin, D. Y., Huang, Y. S., Jeng, J. C., Kuo, H. Y., Chang, C. C., Chao, T. T., Ho, C. C., Chen, Y. C., Lin, T. P., Fang, H. I., Hung, C. C., Suen, C. S., Hwang, M. J., Chang, K. S., Maul, G. G., and Shih, H. M. (2006) Role of SUMO-interacting motif in Daxx SUMO modification, subnuclear localization, and repression of sumoylated transcription factors. *Mol. Cell* **24,** 341–354
50. Weisshaar, S. R., Keusekotten, K., Krause, A., Horst, C., Springer, H. M., Göttsche, K., Dohmen, R. J., and Praefcke, G. J. (2008) Arsenic trioxide stimulates SUMO-2/3 modification leading to RNF4-dependent proteolytic targeting of PML. *FEBS Lett.* **582,** 3174–3178
51. Lallemand-Breitenbach, V., Jeanne, M., Benhenda, S., Nasr, R., Lei, M., Peres, L., Zhou, J., Zhu, J., Raught, B., and de Thé, H. (2008) Arsenic degrades PML or PML-RARα through a SUMO-triggered RNF4/ubiquitin-mediated pathway. *Nat. Cell Biol.* **10,** 547–555
52. Bruderer, R., Tatham, M. H., Plechanovova, A., Matic, I., Garg, A. K., and Hay, R. T. (2011) Purification and identification of endogenous poly-SUMO conjugates. *EMBO Rep.* **12,** 142–148
53. Conlan, L. A., McNees, C. J., and Heierhorst, J. (2004) Proteasome-dependent dispersal of PML nuclear bodies in response to alkylating DNA damage. *Oncogene* **23,** 307–310
54. Brouwer, A. K., Schimmel, J., Wiegant, J. C., Vertegaal, A. C., Tanke, H. J., and Dirks, R. W. (2009) Telomeric DNA mediates *de novo* PML body formation. *Mol. Biol. Cell* **20,** 4804–4815
55. Hendriks, I. A., Treffers, L. W., Verlaan-de Vries, M., Olsen, J. V., and Vertegaal, A. C. (2015) SUMO-2 orchestrates chromatin modifiers in response to DNA damage. *Cell Rep.* **10,** 1778–1791
56. Dellaire, G., and Bazett-Jones, D. P. (2004) PML nuclear bodies: dynamic sensors of DNA damage and cellular stress. *Bioessays* **26,** 963–977
57. Guo, A., Salomoni, P., Luo, J., Shih, A., Zhong, S., Gu, W., and Pandolfi, P. P. (2000) The function of PML in p53-dependent apoptosis. *Nat. Cell Biol.* **2,** 730–736
58. Wang, Z. G., Ruggero, D., Ronchetti, S., Zhong, S., Gaboli, M., Rivi, R., and Pandolfi, P. P. (1998) PML is essential for multiple apoptotic pathways. *Nat. Genet.* **20,** 266–272
59. Wiltshire, T. D., Lovejoy, C. A., Wang, T., Xia, F., O'Connor, M. J., and Cortez, D. (2010) Sensitivity to poly(ADP-ribose) polymerase (PARP) inhibition identifies ubiquitin-specific peptidase 11 (USP11) as a regulator of DNA double-strand break repair. *J. Biol. Chem.* **285,** 14565–14571
60. Schoenfeld, A. R., Apgar, S., Dolios, G., Wang, R., and Aaronson, S. A. (2004) BRCA2 is ubiquitinated *in vivo* and interacts with USP11, a deubiquitinating enzyme that exhibits prosurvival function in the cellular response to DNA damage. *Mol. Cell. Biol.* **24,** 7444–7455
61. Burkhart, R. A., Peng, Y., Norris, Z. A., Tholey, R. M., Talbott, V. A., Liang, Q., Ai, Y., Miller, K., Lal, S., Cozzitorto, J. A., Witkiewicz, A. K., Yeo, C. J., Gehrmann, M., Napper, A., Winter, J. M., Sawicki, J. A., Zhuang, Z., and Brody, J. R. (2013) Mitoxantrone targets human ubiquitin-specific peptidase 11 (USP11) and is a potent inhibitor of pancreatic cancer cell survival. *Mol. Cancer Res.* **11,** 901–911
62. Sowa, M. E., Bennett, E. J., Gygi, S. P., and Harper, J. W. (2009) Defining the human deubiquitinating enzyme interaction landscape. *Cell* **138,** 389–403
63. Wu, H. C., Lin, Y. C., Liu, C. H., Chung, H. C., Wang, Y. T., Lin, Y. W., Ma, H. I., Tu, P. H., Lawler, S. E., and Chen, R. H. (2014) USP11 regulates PML stability to control Notch-induced malignancy in brain tumours. *Nat. Commun.* **5,** 3214